Journal of Physics: Conference Series **1596** (2020) 012047 doi:10.1088/1742-6596/1596/1/012047

Development of a beam profile monitor based on silicon strip sensors for low-charge electron beams

S Jaster-Merz[1,2], R W Assmann[1], F Burkart[1], U Dorda[1], J Dreyling-Eschweiler[1], L Huth[1], U Krämer[1] and M Stanitzki[1]

[1] DESY, 22607 Hamburg, Germany
[2] Institut für Experimental Physik, Universität Hamburg, 22761 Hamburg, Germany

E-mail: sonja.jaster-merz@desy.de

Abstract. Novel accelerator techniques such as dielectric laser acceleration (DLA) will be studied at the SINBAD facility (DESY Hamburg) using the ARES electron linac. Due to the low charge of the accelerated beams, charge densities below 1 aC per square micron are expected at the spectrometer screen, which are challenging to measure with conventional techniques used in multi-pC accelerators. Therefore, a dedicated beam profile monitor, based on silicon strip sensors from the ATLAS inner tracker upgrade, was developed to measure these distributions with a sufficient spatial resolution of around 100 micron. Here, the design of the device and experimental tests with a prototype are presented.

1. Introduction

SINBAD (Short and INnovative Bunches and Accelerators at DESY) [1] is a dedicated accelerator R&D facility at DESY hosting the ARES (Accelerator Research Experiment at SINBAD) linear accelerator [2]. It is currently under commissioning and has been designed to produce ultrashort electron bunches with fs to sub-fs duration [3] for a variety of applications, including injection into novel accelerators. To measure the beam energy at ARES and determine the performance of the novel acceleration techniques under study, a spectrometer setup will be used. This device consists of a dipole magnet and a beam profile monitor which needs to have sufficient sensitivity to spatially resolve the beam. This is a critical point for certain acceleration setups such as dielectric laser accelerators (DLAs), where the produced beams typically feature a low, sub-pC charge, and a possible working point at ARES showed less than 7 electrons per μm^2 at the beam profile monitor location. Such distributions are challenging to measure with conventional techniques used in multi-pC accelerators.

To overcome this challenge, a dedicated detector setup called STRIDENAS (STRIp DEtector for Novel Accelerators at SINBAD), able to resolve these low-charge beams, was developed. The STRIDENAS project is realised as an internal DESY collaboration and profits from both the detector development expertise and the accelerator knowledge at DESY.

Here, the design as well as feasibility studies are presented.

2. STRIDENAS design

STRIDENAS aims at detecting electrons in an area of 2 cm × 1 cm with a spatial resolution of 100 µm and a dynamic range for incoming electrons between $\sim 10 - 234\,000$ electrons

Table 1. ATLAS12EC miniature sensor specifications [4].

	Unit	**Value**
Material		Silicon
Strip Material Doping		n
Bulk Material Doping		p
Number of Strips		103
Sensor Size	mm × mm	10.02 × 10.02
Strip Pitch	µm	74.5
Sensor Thickness	µm	310

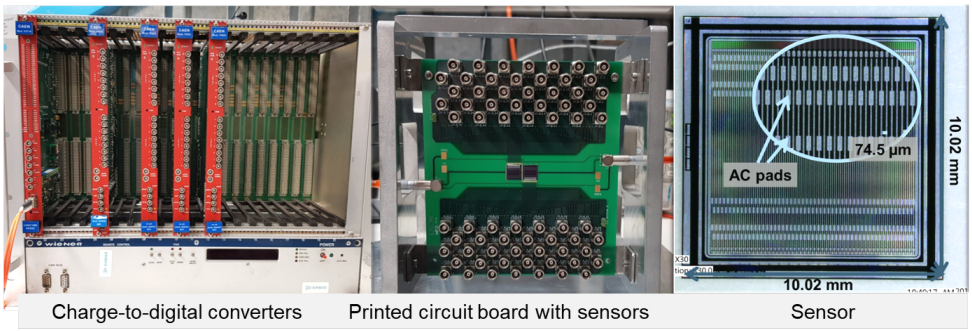

Figure 1. Hardware components of the STRIDENAS detector prototype. Left: CAEN charge-to-digital converters and VME bridge inserted in a VME crate. Middle: Two silicon strip sensors mounted on the STRIDENAS printed circuit board with 64 readout channels. Right: Pictures of the sensor with zoom on the sensor strips and bond pads.

(1.6×10^{-3} fC – 37.5 fC) per 224 µm width. Silicon strip sensors amplify the incoming charge and are designed to detect single minimum ionizing particles (MIPs) in collider experiments. The dynamic range required for STRIDENAS is orders of magnitudes larger, which would saturate the readout electronics used in ATLAS [5] and CMS [6]. It was therefore decided to combine two ATLAS12EC miniature silicon strip sensors [7] with four CAEN charge-to-digital converters (QDCs) of a sufficient high dynamic charge range between 0 pC and 900 pC and a resolution of 200 fC [8]. The strip sensors are glued and bonded to a printed circuit board which connects to the QDCs. The QDCs are read out via an optical fibre, sending data to a PCIe card which is read out by dedicated software. The specifications of the sensors are listed in table 1. Further technical details and more detailed information on the detector design is available in the references [9] and [10]. The three hardware components are shown in figure 1, a sketch of the readout chain is shown in figure 2.

To investigate the impact of a possible transverse signal spread expected for high charge carrier densities [11], a transverse signal spread was simulated using ROOT [12] packages. In addition, transient-current technique measurements with high intensity incoming photon beams were performed. The results are presented in [10] and show no critical behaviour of a transverse signal spread from one sensor strip to its neighbouring one.

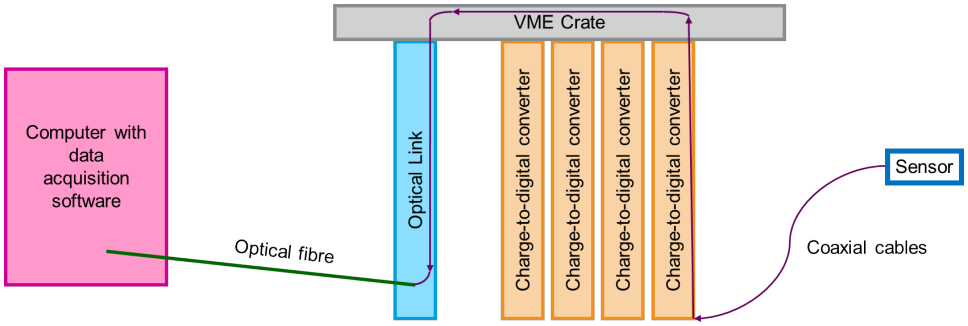

Figure 2. Diagram of the readout chain. The charge-to-digital converters are connected to and controlled by an optical link via the VME crate. The computer containing the data acquisition software is connected to the optical link via an optical fibre.

3. STRIDENAS prototype characterization with beam

Functionality tests of the STRIDENAS components were performed using the DESY II Test Beam Facility [13]. It delivers single electrons for detector tests with energies between 1 GeV and 6 GeV at a particle rate up to 40 kHz. Due to the single incoming electrons, the produced charge in the STRIDENAS detector is very small. It was therefore decided to test the different components individually. The readout electronics were tested using signals produced by photomultipliers, the sensor signals were analysed using an oscilloscope and an additional amplifier. The results of the measurements are presented below.

3.1. Readout electronics

The readout electronics were tested using a signal from a BC408 scintillator of 3 mm thickness [14] which was directly coupled to a Hamamatsu photomultiplier [15] and placed in the electron beam of the Test Beam Facility. In addition, iron plates of different thickness were placed in the beam to produce a particle shower, increasing the number of incoming particles. As an example, a measurement with one iron plate of 2 cm thickness and a charge integration gate of 1 µs is shown in figure 3, where the value on the horizontal axis corresponds to the acquired charge by the charge-to-digital converter in units of ADC counts. The recorded data was fitted between ADC channel 288 and 520 with a superposition of three Landau functions. This fit function was chosen to represent the three visible peaks, which are expected to correspond to one, two and three particle events, assuming the deposited energy follows a Landau distribution, as expected from theory [16]. This is shown in figure 3 where an equally, within the uncertainties, spaced peak structure can be seen. The distance between the first and second peak is (75.7 ± 2.5) ADC Channels, the distance between the second and third peak is (77.5 ± 5.9) ADC Channels. Assuming 200 fC per ADC Channel this results in a spacing of (15.1 ± 0.5) pC and (15.5 ± 1.2) pC, respectively.

Assuming a photomultiplier gain of 2×10^5 [15], a scintillator light yield of $\sim$ 1600 photons per mm and per incoming MIP and an efficiency of 10 % [17], the produced charge per incoming MIP after the photomultiplier can be roughly estimated to be 15 pC. This agrees well with the peak spacing measured with the QDC.

3.2. Sensor with amplifier

Functionality tests of the sensor were performed using 2 GeV and 4 GeV electrons from the DESY II Test Beam and a Tektronix MSO 5104B oscilloscope [18] for the readout. First measurements with the STRIDENAS detector were unsuccessful due to an early breakdown of the sensors [10].

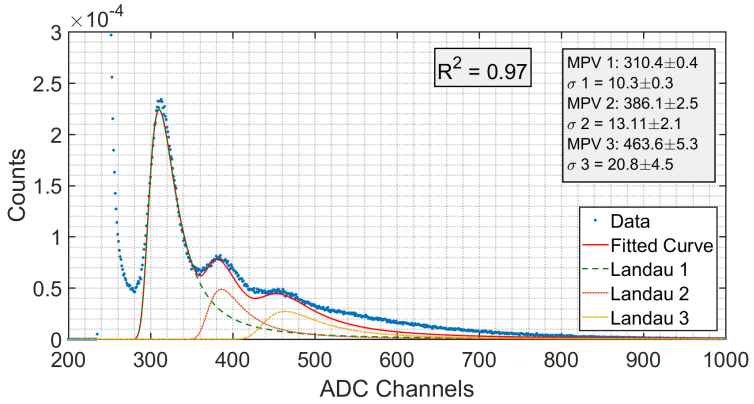

Figure 3. Triple Landau distribution fit to the photomultiplier data measured with the charge-to-digital converter and one shower plate for a 1 µs charge integration gate. The data is displayed in a linear range and normalized to the total number of recorded events.

Table 2. Femto HSA-X-1-40 amplifier specifications [19].

Parameter	**Unit**	**Value**
Gain	dB	40 ± 1
Impedance	Ω	50
Bandwidth	kHz	10 - 1200000
Rise time	ps	290

Measurements with a functional sensor on another PCB were successful. A bias voltage of $-290\,\mathrm{V}$ was applied to the sensor which corresponds to the measured depletion voltage of the sensor [10]. The produced charge inside the sensor however was too small to be detected and no signal from the Test Beam was visible. Further measurements of the sensor with a Femto HSA-X-1-40 [19] 40 dB amplifier were performed. The specifications of the amplifier are listed in table 2. A recorded signal is shown in figure 4.

The area of the sensor signal is proportional to the produced charge inside the sensor and varies, following an expected Landau distribution. To obtain the area under the signal, a baseline correction was performed and the signals were integrated. The integration boundaries were determined relatively to the peak position between $-5 \times 10^{-10}\,\mathrm{s}$ and $5\,\sigma$ after the peak. The σ is the standard deviation of the peak which was obtained by calculating the standard deviation of all data points between $-5 \times 10^{-10}\,\mathrm{s}$ and $10^{-7}\,\mathrm{s}$ with a value smaller than $-0.01\,\mathrm{V}$.

A histogram of the signal integrals for all recorded signals and a fit for the Landau distribution is shown in figure 5. The integral values agree well with the Landau distribution as can be seen by the factor R^2 of 0.97. The most probable value (MPV) obtained from the fit can be used as an integral equivalent to the most probable charge produced in the sensor which can be calculated from the data as

$$Q = \frac{L_c}{A \cdot R} \cdot \int_{t_\mathrm{s}}^{t_\mathrm{f}} U dt \sim \frac{L_c}{A \cdot R} \cdot I_M \cdot \Delta t, \tag{1}$$

where L_c is the compensation for signal losses in the cable, A is the amplification factor of the amplifier, R is the impedance of the system and U is the measured voltage, which is integrated

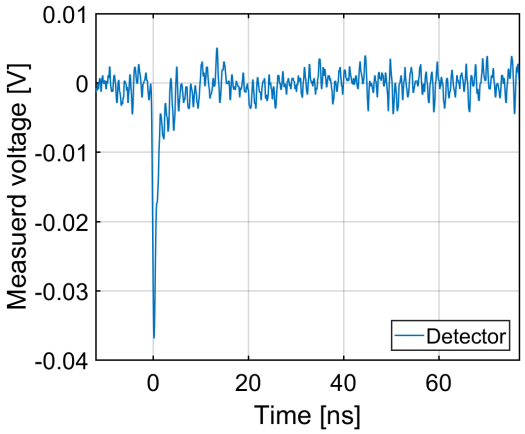

Figure 4. Example of a recorded waveform from the sensor in combination with a 40 dB amplifier. The spike corresponds to the detected signal from a particle.

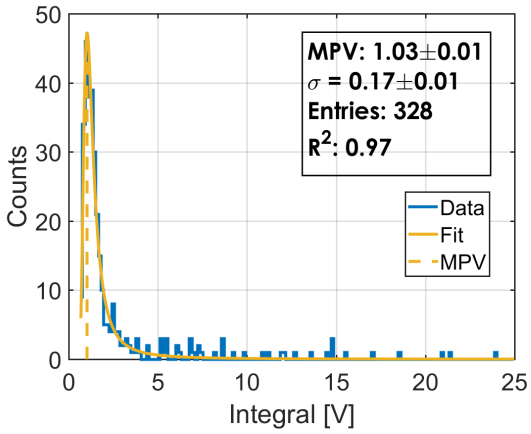

Figure 5. Histogram of the waveform integrals and fit of a Landau distribution. The integral values correspond to the integral I_M described in (1).

Table 3. Parameters and uncertainties used for the most probable charge production calculation in the sensor.

Parameter	**Unit**	**Value**	**Uncertainty**
Integral I_M	V	1.03	0.13
Timestep Δt	s	5.17×10^{-11}	–
Impedance R	Ω	50	–
Amplification A	dB	40	1
Loss compensation L_c		1.07	–

between the starting and final time boundaries t_s and t_f. This integral was calculated with a MATLAB function which assumes a unitary spacing between data point. Therefore, the obtained integral value, I_M, has to be multiplied by the actual data spacing Δt. Impedance mismatch and changes in the time steps (sampling rate of oscilloscope) were neglected.

The most probable charge produced inside the sensor was determined by using (1). For the integral value, the most probable value obtained from the Landau fit was used. All parameters and uncertainties are listed in table 3. With these values, the average charge produced in the sensor was found to be

$$Q = (1.14 \pm 0.14) \cdot 10^{-14}\ \mathrm{C}. \tag{2}$$

The number of produced electron-hole pairs per µm sensor thickness can be obtained by dividing Q over the thickness of the sensor d_{sensor} and the electron charge e

$$\mathrm{N_{e\text{-}h}} = \frac{Q}{d_{\mathrm{sensor}} \cdot e}. \tag{3}$$

For the ATLAS12EC miniature sensor with a thickness of 310 ± 25 µm this results in

$$\mathrm{N_{e\text{-}h}} = (229 \pm 34)\ \text{electron-hole pairs per µm}. \tag{4}$$

This value is ~ 2.7 times higher than the average of 80 electron-hole pairs per µm produced by a MIP [16]. This discrepancy might occur due to an imprecise signal loss compensation L_c, a possible impedance mismatch, noise fluctuations mainly due to ~ 30 cm long cables between sensor and amplifier, errors in the signal integral or additionally incoming low energetic shower particles.

4. Conclusion

First proof-of-principle tests with the STRIDENAS sensor at the DESY II Test Beam Facility showed that single electron detection is possible with the sensor even when it is not used in combination with its usual readout electronics. Previously performed high intensity measurements with a high intensity, infrared laser beam looked promising and showed no impact of a transverse signal spread. The STRIDENAS readout electronics were successfully tested with high intensity signals from a photomultiplier.

5. Outlook

As a next step, further sensor tests using a high intensity electron beam with up to 10^{10} electrons per bunch are foreseen. Such measurements could, for example, be performed inside the DESY II tunnel at DESY Hamburg and have the advantage of investigating the sensor and signal behaviour under realistic conditions. In addition, the development of a suited amplification system for all readout channels is foreseen to reduce the impact of noise which is mainly introduced by several meter long cables.

For the final implementation of the STRIDENAS detector at the ARES beamline a vacuum compatible design is needed. Discussions with the DESY vacuum group are ongoing and include, for example, the change to a ceramic based printed circuit board.

Acknowledgments

The measurements leading to these results have been performed at the Test Beam Facility at DESY Hamburg (Germany), a member of the Helmholtz Association (HGF).

References

[1] Dorda U *et al.* 2018 *Nucl. Instr. Meth.* **909** 239–242
[2] Marchetti B *et al.* 2016 Technical Design Considerations About the SINBAD-ARES Linac *Proc. 7th Int. Particle Accelerator Conf. (IPAC'16)* 7 (Busan, Korea) pp 112–114 URL doi:10.18429/JACoW-IPAC2016-MOPMB015
[3] Zhu J, Assmann R W, Dohlus M, Dorda U and Marchetti B 2016 *Phys. Rev. Accel. Beams* **19**(5) 054401 URL doi:10.1103/PhysRevAccelBeams.19.054401
[4] ATLAS Upgrade Strip Sensor Collaboration *et al.* 2012 Supply of Silicon Microstrip Sensors of ATLAS12EC Specification Tech. rep.
[5] ATLAS Collaboration 2017 Technical design report for the ATLAS inner tracker strip detector Tech. rep.
[6] Karimäki V 1997 The CMS tracker system project: Technical Design Report Tech. rep. CMS-TDR-005
[7] Unno Y *et al.* 2011 *Nucl. Instr. Meth.* **636** S24–S30
[8] CAEN *Technical Information Manual* **29**
[9] Jaster-Merz S, Assmann R W, Burkart F, Dorda U, Kraemer U, Panofski E and Stanitzki M 2019 *Journal of Physics: Conference Series* **1350** 012148
[10] Jaster-Merz S 2019 *Magnet Characterization and Beam Profile Monitor Development for a Spectrometer at the ARES Linac* Mastersthesis University of Hamburg URL https://bib-pubdb1.desy.de/record/425405
[11] Becker J, Eckstein D, Klanner R and Steinbrueck G 2010 *Nucl. Instr. Meth.* **615** 230–236
[12] Brun R and Rademakers F 1997 *Nucl. Instr. Meth.* **389** 81–86
[13] Diener R *et al.* 2019 *Nucl. Instr. Meth.* **922** 265–286
[14] Description of hardware components of the DESY Telescopes accessed: 2019-12-19 URL https://telescopes.desy.de/Hardware
[15] Hamamatsu Photosensor Modules H11900/H11901 series accessed: 2019-06-17 URL https://www.hamamatsu.com/resources/pdf/etd/H11900_H11901_TPMO1076E.pdf

[16] Spieler H 2005 *Semiconductor Detector Systems* vol 12 (Oxford university press)
[17] Marcel Stanitzki and Katja Krüger 2019 private communication
[18] MSO5000B, DPO5000B Series Datasheet `https://de.tek.com/datasheet/mixed-signal-oscilloscopes` accessed: 2019-06-30
[19] Datasheet Femto HSA-X-1-40 `https://www.femto.de/images/pdf-dokumente/de-hsa-x-1-40.pdf` accessed: 2019-06-23